Supporting Online Material for

Mapping Nanoscale Variations in Photochemical Damage of Polymer/Fullerene Solar Cells with Dissipation Imaging

Phillip A. Cox, Dean A. Waldow, Torin J. Dupper, Stephen Jesse, David S. Ginger*

*To whom correspondence should be addressed: ginger@chem.washington.edu

1. Comparison Between EQE and Absorption Loss

To illustrate the increased reduction in EQE versus absorption, we plot the percent change in EQE (at 450 nm) and absorption (also at 450 nm) as a function of *absorbed* photon dose in Figure S1. The EQE at each dose is referenced to the fresh device EQE. The absorbed photon dose corrects for the loss in absorbance of the film as it degrades.

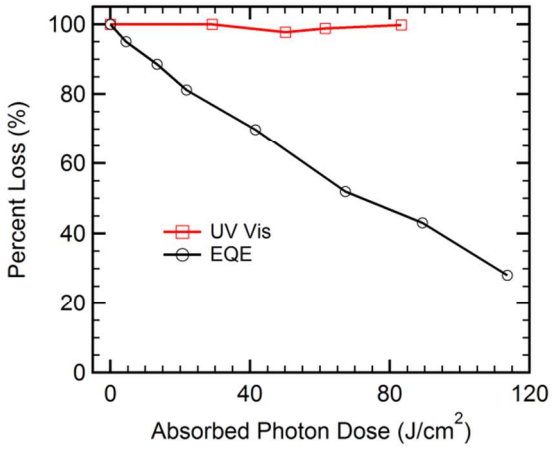

Figure S1. Percent change of UV-Vis and EQE (at 450 nm) for 3% PTB7:$PC_{71}BM$ devices as a function of absorbed photon dose. The absorbed photon dose accounts for loss in absorbance as the devices degrade.

2. Band Excitation Data: Relationship of Q to FM-EFM Amplitude

To show that amplitude measured via FM-EFM is proportional to Q measured via Band Excitation (BE), we photo-oxidized a 3% DIO PTB7:$PC_{71}BM$ sample through a TEM Grid (PELCO 400 Mesh) to create a sharp step between fresh and degraded areas in the film. We degraded the sample to a photon dose of ~400 J/cm^2 using a 660 nm 5 W LED (LEDEngin LZ10R200). We imaged the sample using FM-EFM and BE on an Asylum Cypher AFM at the Center for Nanophase Materials sponsored by Oak Ridge National Laboratory. Like our measurements on the MFP-3D BIO system, we applied +10 V to the tip at a lift height of 10 nm during FM-EFM imaging. Due to difficulties with the particular BE hardware used, we applied a tip bias of +7.5 V. Regardless, the images show that cantilever amplitude is proportional to cantilever Q under our imaging conditions.

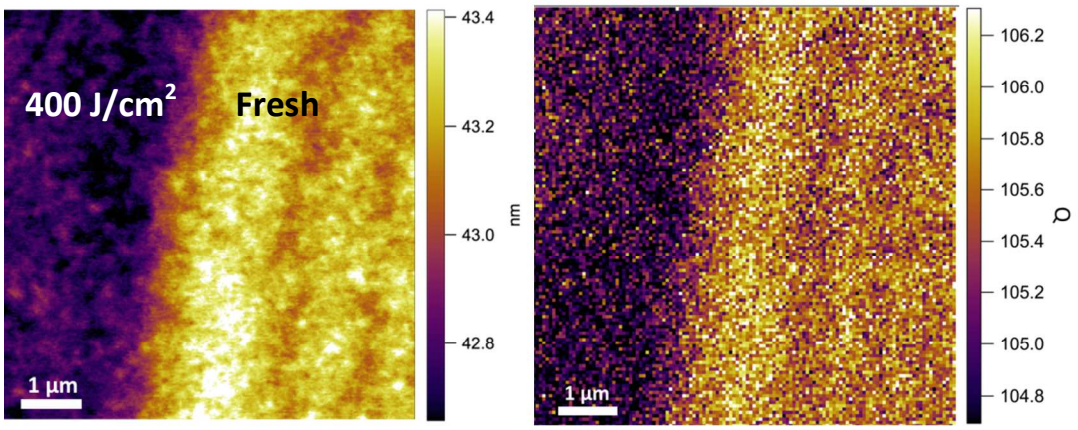

Figure S2. A comparison between (A) amplitude from FM-EFM and (B) Q from Band Excitation for a 3% DIO PTB7:$PC_{71}BM$ sample photodegraded through a TEM grid using cw 660 nm light.

We report FM-EFM amplitude images as ΔQ/Q to account for variations in drive amplitude from image to image. ΔQ/Q is equivalent to ΔA/A and eliminates the need to measure drive amplitude:

$$\frac{\Delta Q}{Q} = \frac{Q_{eff} - Q_{avg}}{Q_{eff}} = \frac{\frac{A_{eff}}{A_d} - \frac{A_{avg}}{A_d}}{\frac{A_{eff}}{A_d}} = \frac{\frac{A_{eff} - A_{avg}}{A_d}}{\frac{A_{eff}}{A_d}} = \frac{A_{eff} - A_{avg}}{A_{eff}} = \frac{\Delta A}{A} \qquad (1)$$

Here, A_d is the drive amplitude, Q_{eff} and A_{eff} are Q and amplitude of the cantilever at any given pixel in the image, while Q_{avg} and A_{avg} are the average Q and amplitude over the fresh areas of the device. In the case of films photo-oxidized with spots by the HeNe laser, the average amplitude excludes the degraded areas.

3. Sensitivity of Q-Imaging in Photo-Oxidative Studies

To provide evidence for the sensitivity of Q-imaging compared to SKPM in photodegraded OPVs, we carried out an additional *in situ* photo-oxidation experiment where a sample was exposed to a 633 nm HeNe laser (5 mW Research Electro-Optics) at ~5030 W/m^2 for photon doses ranging from ~600 to 3000 J/cm^2. SKPM images were taken both in the dark and under 660 nm illumination (5060 W/m^2 LEDEngin). Even for doses up to 3000 J/cm^2, differences in sample work function are difficult to discern.

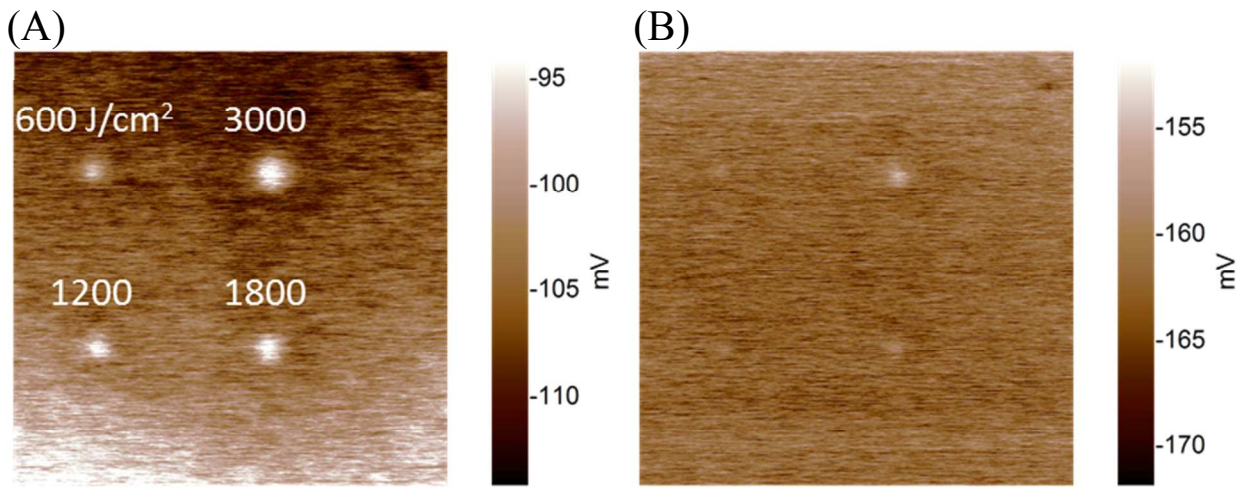

Figure S3. Changes in tip bias measured via amplitude-feedback SKPM for a 3% DIO PTB7:$PC_{71}BM$ sample photo-oxidized *in situ* with cw 633 nm laser at ~5030 W/m^2 for photon doses ranging from ~600 to 3000 J/cm^2 in (A) dark and (B) 660 nm illumination. Images are 20x20 microns.

On the same sample in Figure S3, we collected a ΔQ/Q image to show that when the sample is degraded past its functional lifetime, the sign of ΔQ/Q changes and Q begins to rise in the degraded areas. At high enough doses, Q actually exceeds that of a fresh film. This is important to note as it essentially means the relationship between ΔQ/Q and external quantum efficiencies that we show in Figure 3 breaks down once the device has been degraded past normal functionality. Care must be taken in degrading to reasonable photon doses when comparing local FM-EFM results with bulk device measurements.

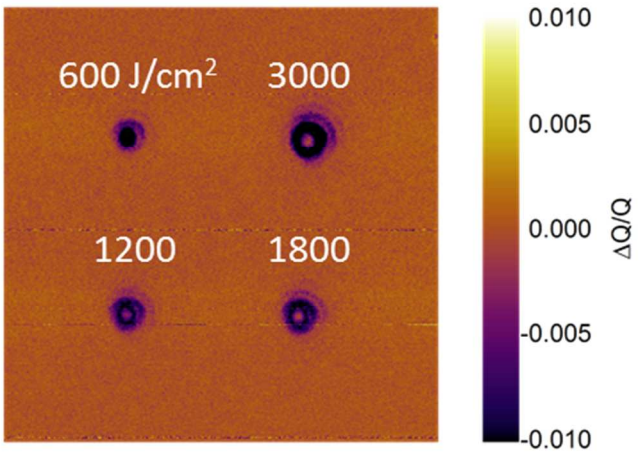

Figure S4. The ΔQ/Q image of a 3% DIO PTB7:$PC_{71}BM$ sample photo-oxidized *in situ* with cw 633 nm laser at ~5030 W/m^2 for photon doses ranging from ~600 to 3000 J/cm^2. Image is 20x20 microns.

4. Table of Cantilever Constants

	Resonance Frequency	Spring Constant	Quality Factor*
Multi75-G	75 ± 15 kHz	3 N/m	164
Tap190-G	190 ± 60 kHz	48 N/m	391
Tap300-G	300 ± 100 kHz	40 N/m	508

Table S1: Manufacturer reported constants for the cantilevers used in this study.
*Experimentally determined.

4. Additional Images

The photo-oxidation images shown in Figure 5 and Figure 6 were also taken at higher photon doses (800, 1200, 1800, and 3000 J/cm^2) to assess the evolution of photochemical damage throughout the lifetime of the device. We chose to display only the fresh and 400 J/cm^2 images to highlight the most important differences between PTB7:$PC_{71}BM$ films made with and without DIO. Figure S5 (DIO) and Figure S6 (no DIO) show the images over the entire range of photon dose.

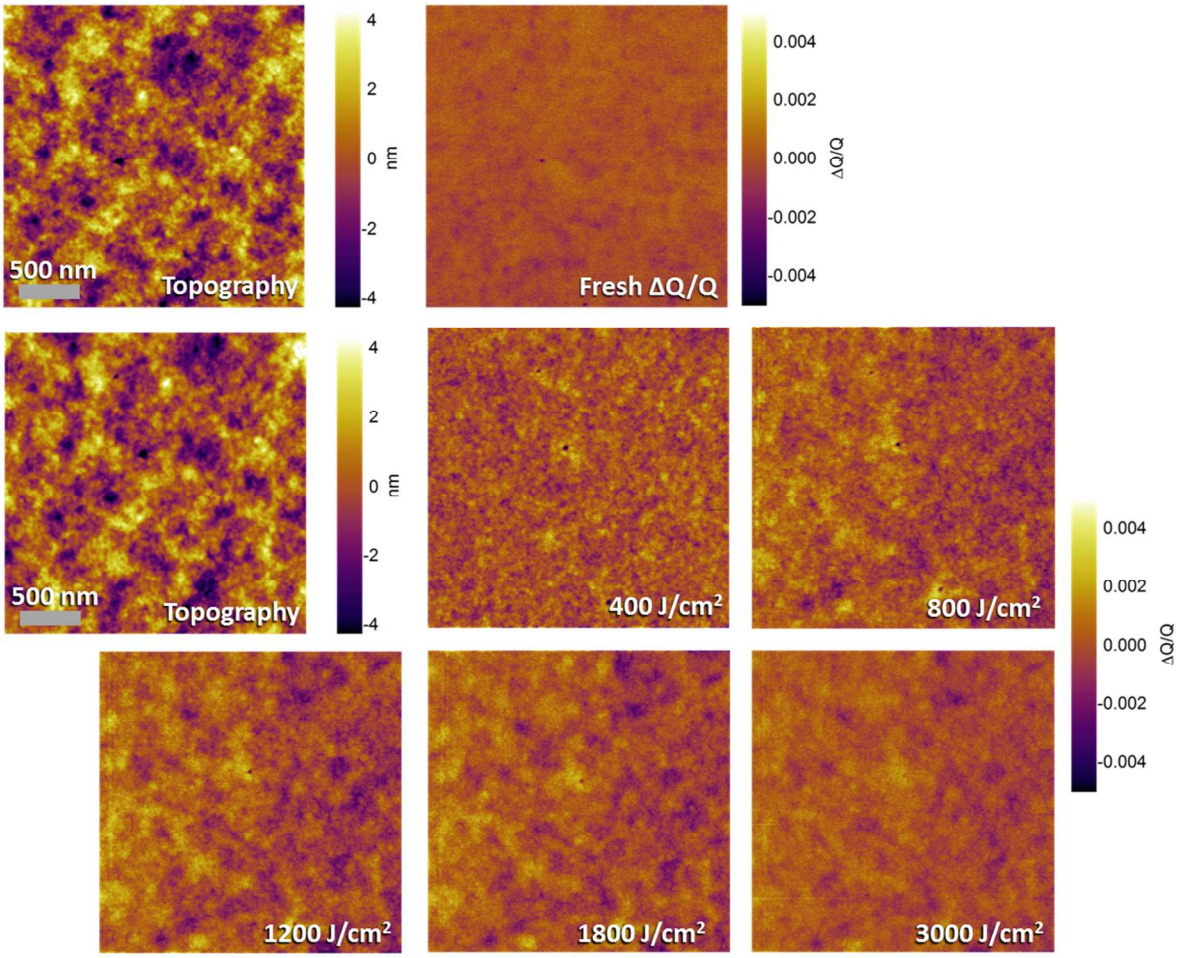

Figure S5. Topography and ΔQ/Q for all photon doses (0, 400, 800, 1200, 1800, 3000 J/cm^2) of a 3% DIO PTB7:$PC_{71}BM$ film photo-oxidized *in situ* with a 660 nm LED.

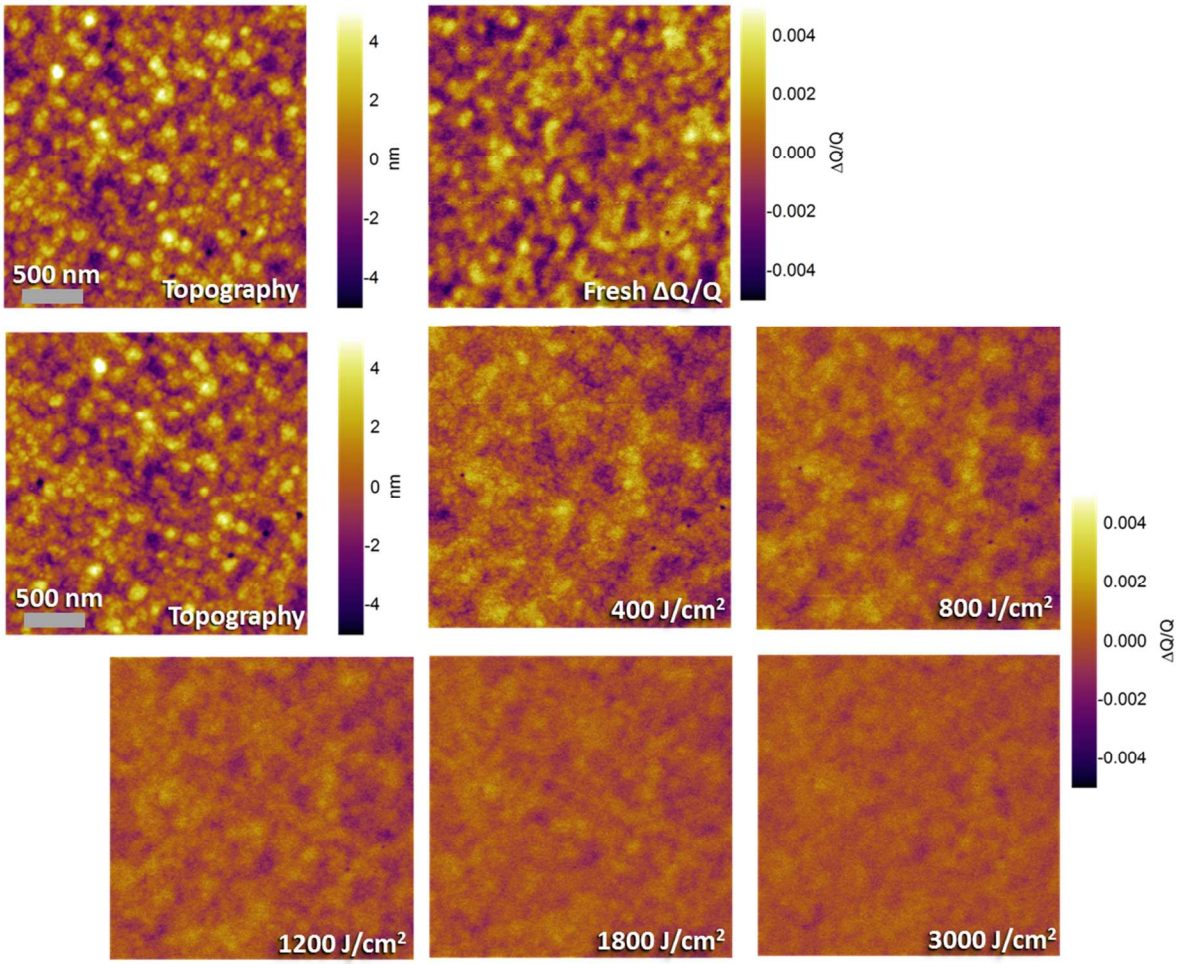

Figure S6. Topography and ΔQ/Q for all photon doses (0, 400, 800, 1200, 1800, 3000 J/cm^2) of a 0% DIO PTB7:$PC_{71}BM$ film photo-oxidized *in situ* with a 660 nm LED.

5. Evolution of Q Distribution in PTB7:$PC_{71}BM$ Films Processed With and Without DIO

To more quantitatively assess the distribution of Q changes seen in photo-oxidizing PTB7:$PC_{71}BM$ films processed with and without DIO, we fit a histogram of flattened FM-EFM amplitude images from figures S5 and S6 (not converted to ΔQ/Q in this case) with a Gaussian and then plotted the value of the Gaussian width of each image against photon dose. The greater the variation in tip amplitude over the image, the greater the Gaussian width (i.e. a uniformly performing device would have a very small Gaussian width).

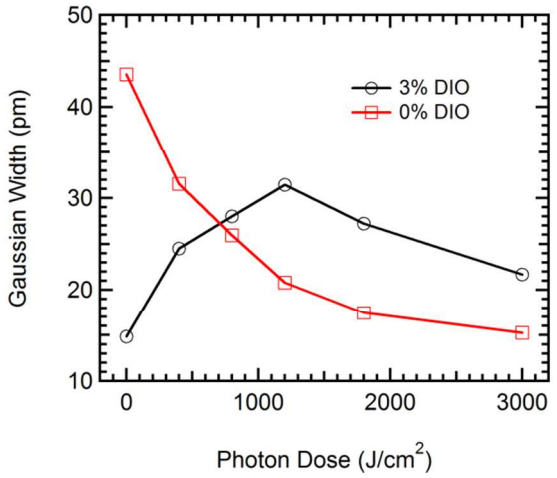

Figure S7. Distribution of amplitudes measured by FM-EFM as a function of photon dose for PTB7:$PC_{71}BM$ films processed with and without DIO.

6. Comparison between 0% and 3% DIO PTB7:$PC_{71}BM$ EQEs as a function of photon dose.

We show in Figure S8 and Figure S9 the difference in stabilities between PTB7:$PC_{71}BM$ devices processed with and without DIO. Devices processed without DIO degrade at a faster rate. We note that the devices made with 0% DIO were fabricated using a different batch of PTB7 polymer from 1-Material and, despite the exact same processing conditions, resulted in a higher performing device. We do not believe this affects the stability of the devices. Figure S9 shows the percent loss in EQE as a function of photon dose for both 0% and 3% DIO devices. We did this by calculating the %-difference from the fresh device for each photon dose and then plotting it against the *absorbed* photon dose. The absorbed photon dose corrects for the loss in absorbance of the film as it degrades.

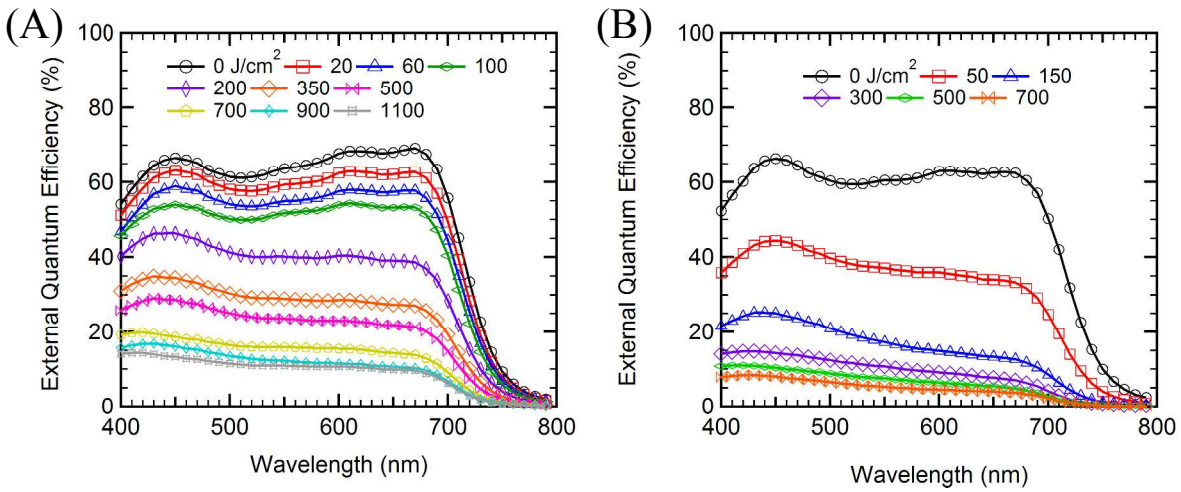

Figure S8. External quantum efficiencies of PTB7:$PC_{71}BM$ processed (A) with and (B) without DIO photo-oxidized over photon doses ranging from 0 to 1100 J/cm^2.

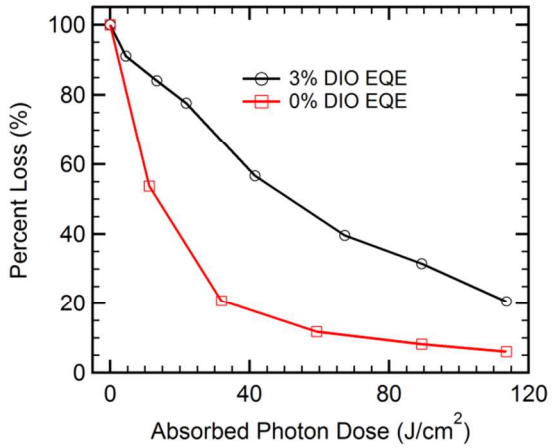

Figure S9. A comparison between the % change in EQE at 660 nm of 0% and 3% DIO PTB7:$PC_{71}BM$ devices as they are subjected to increasing photon doses.